31st Annual International Conference of the IEEE EMBS
Minneapolis, Minnesota, USA, September 2-6, 2009

A Morphologically Realistic Shell Model of Atrial Propagation and Ablation

Amr Al Abed *Member IEEE*, Socrates Dokos, and Nigel H. Lovell, *Senior Member, IEEE*

Abstract— **A three dimensional morphologically realistic model of atrial propagation is developed, based on the male Visible Human dataset and the Fitzhugh-Nagumo equations for cardiac excitation. The atrial shell geometry incorporates eleven different anatomical structures, including the pulmonary veins, and the septum, Bachmann's bundle and coronary sinus as interatrial conduction pathways. Although the model utilizes a simplified cellular model of cardiac excitation it is able to reproduce a variety of electrophysiological phenomena including: autorhythmicity of the sinoatrial node and its ability to excite surrounding atrial tissue, spiral re-entrant wavefronts, ectopic beats originating in the PV and their termination by circumferential ablation of the PV. The model is an important tool to quantitatively study atrial excitation under normal conditions and during atrial fibrillation.**

I. Introduction

Atrial fibrillation is a common condition affecting the elderly population and strongly correlated with the incidence of stroke [1]. It is caused by abnormal atrial activation and/or disturbances to the rhythmic propagation of electrical impulses in the atria, leading to the formation of re-entrant wavefronts. The underlying factors initiating atrial fibrillation are not completely understood but include ectopic sources of spontaneous electrical activity that can trigger re-entrant wavefronts [1]. Over the last 10-15 years the treatment for atrial fibrillation has extended to direct ablation of ectopic foci or electrically isolating these using radiofrequency-induced lesions based on the Cox Maze surgical procedure [2], or Haissaguerre's approach of isolating the PVs [3]. However, identification of the optimum ablation procedure is currently based largely on empirical clinical approaches.

Computer simulation of atrial excitation is an important approach that offers insights into normal and abnormal electrical propagation in the atria. It can be also used to quantitatively study the various factors contributing to the genesis and maintenance of re-entrant wavefronts, assess the efficacy of various ablation procedures and help identify optimal ablation sites for each pathophysiology; a further step towards patient specific therapy. In order to achieve this aim, the computer models should be based on anatomically accurate atrial geometries.

The authors would like to thank Andrew Sims for valuable image reconstruction and mesh generation tips. A. Al Abed is a PhD candidate at the Graduate School of Biomedical Engineering, the University of New South Wales. S. Dokos and N. H. Lovell are with the Graduate School of Biomedical Engineering, the University of New South Wales, Sydney, 2052, Australia (e-mail: s.dokos@unsw.edu.au).

Over the last decade realistic computer models of atrial electrophysiology have been developed [4], [5]. These models are based on anatomically realistic geometries that incorporate atrial wall thickness to simulate transmural conduction. Although biophysically accurate, they are computationally expensive and thus were only used to simulate short periods of atrial activation and propagation, which is not sufficient to study the behavior of re-entrant waveforms during arrhythmia. To reduce the computational cost, a cellular autonoma approach can be used to model atrial fibrillation and ablation [6]. Alternatively, as the atrial wall is thin, it can be represented by a shell structure. This assumption has been utilized to develop a morphologically realistic shell model of the atria that was applied to study fibrillation [7] and ablation therapy [8].

Our group has previously published a simplified atrial 3D model with a spontaneously active sino-atrial node (SAN) that is able to excite surrounding atrial tissue [9]. In this study a morphologically realistic 3D model of atrial electrophysiology is developed. The novel shell morphology is based on images of a male atrium and includes the atria, major vessels, both atrial appendages, openings for the mitral and tricuspid valves, and the coronary sinus (CS) and Bachmann's bundle (BB) as two interatrial conduction pathways. The SAN and crista terminalis (CT) are defined as distinct surfaces based on their anatomical location and size. Both the myocardium and pulmonary vein (PV) walls are modeled as continuous excitable media. Modified versions of the Fitzhugh-Nagumo equations [10] are used to model the spontaneous rhythmic excitation of the SAN and electrical propagation through the atrial structures and vessel walls. To our knowledge this is the first published anatomically realistic atrial shell model that incorporates a spontaneously active SAN. The incorporation of the PVs and the CS allows the study of their role in atrial fibrillation in a computationally efficient model. In this study the interaction of an ectopic impulse originating in a PV with spontaneous wavefronts initiated at the SAN is investigated. The effect of an ablation lesion on the resultant arrhythmic behavior is also presented.

II. Methods

A. Image Segmentation

Cryosections (0.33mm × 0.33mm × 0.33mm) of the Male Visible Human thorax were obtained from the U.S National Library of Health (Visible Human Project, USA [11]). The raw slices were registered and converted to grayscale images

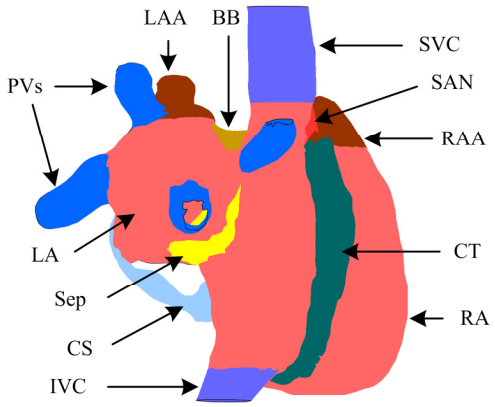

Fig. 1. A posterior-medial view of the atrial Geometry. RA: Right Atrium, LA: left atrium, CT: Crista Terminalis, SAN: sinoatrial node, SVC: Superior Vena Cava,Bachmann's bundle, SCV: Superior Vena Cava, IVC: Inferior Vena Cava, RAA: Right Atrial Appendage, BB: Bachman's Bundles, Sep: Septum, CS: Coronary Sinus, LAA: Left Atrial Appendage, PVs: Pulmonary Vein wall. Note both epicardial and endocardial (through the right inferior PV cavity) views of the septum are shown.

in Matlab (MathWorks Inc., USA) then imported to ScanIP (Simpleware Ltd., Exeter UK) for segmentation.

Initially, the atrial chambers and major blood vessel cavities (PVs, superior vena cava (SVC), inferior vena cava (IVC), and CS) were segmented as a single entity using a 3D floodfill algorithm based on upper and lower intensity threshold values. Histological studies have shown that cardiomyocytes can extend up to 20mm into the PV walls as myocardial sleeves [12]. The four PVs were cropped at their first branching point or at 20mm distal to their intersection with the left atrial chamber, whichever was shorter. The resulting mask was smoothed, downsampled to a resolution of 1mm×1mm×1mm and used as a template for further segmentation work.

It is well established that different regions of the atria have different electrophysiological properties. The template mask was segmented into 11 distinct regions thought to be important in electrical conduction, genesis or maintenance of re-entrant wavefronts, or are sites of ectopic foci (Fig. 1). The PVs, CS, SVC and IVC were manually segmented as separate masks at their contact with the atrial chambers. The septum, CT, right and left atrial appendages, and BB were identified using a 3D floodfill algorithm with the appropriate intensity threshold levels. The sinus node artery was noted in the colored images and used as a landmark, together with the CT, SVC and right atrial appendage masks, to estimate the anatomical location and manually paint a mask of the SAN. The dimensions of the resultant SAN mask [10mm × 5mm × 8mm, surface area 340 mm^2] are within the range of values reported in histological studies [13]. Finally, each mask was individually filtered using a morphological filter and smoothed.

B. Mesh Generation

The segmented masks were used to generate a tetrahedral mesh using ScanFE (Simpleware Ltd., Exeter UK) with all masks meshed simultaneously to ensure proper contact areas. The mesh was imported into the finite element modelling package Comsol Multiphysics (Comsol AB, Sweden) and converted to a shell object with triangular mesh elements.

C. Modeling Atrial Electrophysiology

A monodomain formulation of the Rogers-McCulloch modified Fitzhugh-Nagumo equations [10] were used to model cardiac action potentials (1)-(4). In these equations v is the excitation variable and represents the transmembrane potential, u is an action potential recovery variable and a, c_1, c_2, b, d are gating parameters (selected by trial and error). The equations were scaled to produce physiologically realistic action potential duration, amplitude, and resting membrane potential using factors A, B, k and e [9]. All parameters are listed in table 1 in [9].

$$\nabla.\sigma\nabla v = \frac{dv}{dt} + I_{ion} \quad (1)$$

$$\frac{du}{dt} = ke\left(\frac{v-B}{A} - ud - b\right) \quad (2)$$

In this study only the SAN was modeled as having distinct electrophysiological properties. All other surfaces were considered, electrophysiologically, as atrial tissue. The ionic current for atrial cells is given by (3), and modified in (4) to generate spontaneous action potentials in SAN cells [9].

$$I_{ion,atr} = k\left(c_1(v-B)\left(\frac{v-B}{A} - a\right)\left(1 - \frac{v-B}{A}\right) - c_2u(v-B)\right) \quad (3)$$

$$I_{ion,SAN} = k\left(c_1(v-B)\left(\frac{v-B}{A} - a\right)\left(1 - \frac{v-B}{A}\right) - c_2u\right) \quad (4)$$

The tissue conductivity (σ) value was empirically determined to reflect physiologically realistic values of conduction in the human atria (of the order of 0.1 $m.s^{-1}$). Isotropic and homogenous tissue conductivity was assumed for all regions. The transition from myocardium to smooth muscle in the PVs, SVC and IVC walls was modeled by imposing a Dirichlet boundary condition (v = -85 mV) at the outer edges of the PVs, SVC and IVC. Neumann boundary conditions were imposed at the edges of the mitral and tricuspid valve openings. The model was solved for 92789 degrees of freedom using a direct PARDISO solver on a windows 64-bit server with 128GB of RAM and utilizing 4 processors. It took ~17 minutes to solve a 1 s simulation.

D. Modeling Arhythmias and Ablation

The site of ectopic activity was assigned by manually selecting an arbitrary area on the PV wall and pacing it using a suprathreshold stimulus. It was found that the size of the ectopic region was crucial to initiate an ectopic beat. The area was gradually increased until successful excitation was achieved. An ablation lesion was manually drawn around the junction of the PV and LA. The tissue conductivity of the lesion was set to zero.

III. Results

A. Normal Atrial Activation and Propagation

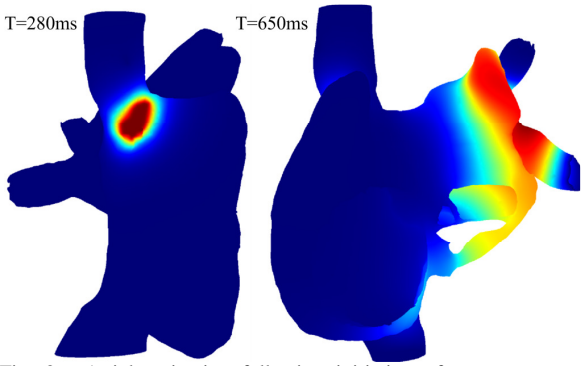

Fig. 2. Atrial activation following initiation of a spontaneous impulse at the SAN (red: v>0mV, dark blue: v<-70mV).

Spontaneous rhythmic impulses were initiated at the SAN and electrotonically activated the surrounding atrial tissue at the anterio-lateral junction of the atrium and SVC (Fig. 2). The initial activation site gave rise to two excitation wavefronts that propagated superiorly and inferiorly. The first compotentent activated the anterio-lateral (25ms) and then posterior-medial (100ms) wall of the SVC in a horsehoe-like fashion. The second wavefront activated the anterio-superior wall of RA (75ms), RAA (125ms) and then propagated inferiorly though the RA. The leading part of the wavefront was always along the CT. The tricuspid isthmus was the last area of the RA to be activated (300ms). The entire RA recovered at 400ms. Inter-atrial conduction was first observed as passive excitation of BB. The first active inter-atrial excitation occurred through the anterior (225ms) and then posterior (250ms) parts of the septum. In the anterior LA the excitation wavefront propagated in an inferior medial to superior lateral direction. From a posterior perspective, the continuation of this wavefront propagated from an inferior medial to superior lateral direction. An excitation wavefront propagated through the CS (300ms) but did not activate left atrial tissue was it was still refractory. The right inferior and superior PVs were activated at 350ms and left inferior PVs and LAA were activated at 375ms followed by the superior left PV (400ms) which was the last LA structure to be activated. The entire LA as fully repolarised 500ms after the initiation of the SAN impulse (Fig. 2).

B. Arrhythmia Simulations

Two types of arrhythmia were induced depending on the location of the ectopic foci. Ectopic impulses originating from the inferior left PV wall activated the PV wall and propagated into LA where they self-terminated. On the other hand, ectopic impulses originating at the inferior of the LA, between its junction with the inferior left PV and septum, interacted with the spontaneous wavefront originating from the SAN to produce a re-entrant spiral that moved in a clockwise direction around both atria (Fig. 3a,b). The spiral activity was only sustained for 500ms. Termination occurred

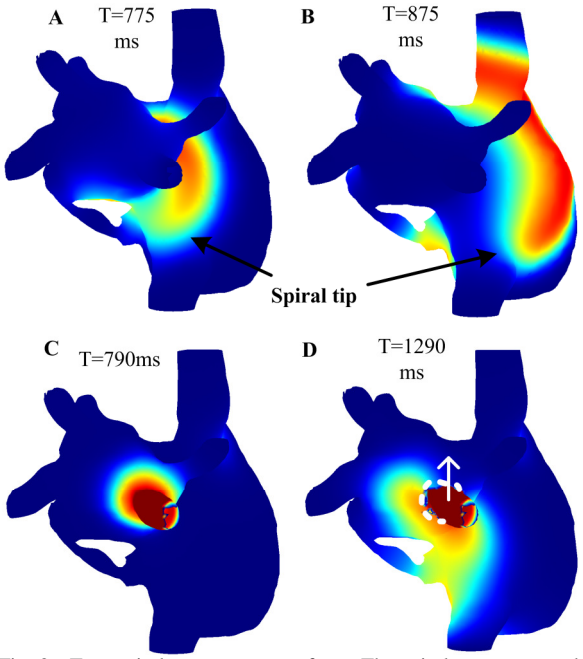

Fig. 3. Top: spiral re-entrant wavefront. The spiral was generated by applying an ectopic stimulus to the inferior LA at t = 750ms. Note that the wavefront moves from the left to right atrium. Bottom: Ectopic impulses propagating from the inferior left PV before (C) and after (D) introducing an ablation lesion (dashed line). Note entrance block (arrow) following ablation. (red: v>0mV, dark blue: v<-70mV).

when the wavefront moved from the RA through the CS but failed to excite the larger left atrial myocardium.

C. Ablation Simulations

Simulations were run to test the ability of an ablation lesion to terminate the propagation of impulses originating from the inferior left PV wall at a frequency of 2Hz (Fig. 3c). An ablation lesion was applied 200ms following the initiation of the first ectopic beat. The ablation lesion prevented propagation of the next ectopic impulse into the LA and the propagation of wavefronts from the LA into the inferior left PV (Fig. 3d).

IV. Discussion and Conclusion

A morphologically-accurate and computationally efficient 3D model of the atria is developed. The model is more anatomically detailed than currently published atrial shell models (e.g. [7], [8]) as it incorporates the PVs, IVC, SVC and CS as distinct structures.

As the model incorporates a SAN of realistic size, location, and electrophysiological properties the site of impulse initiation and pattern of activation of surrounding atrial tissue is comparable to *in vivo* records in humans [14]. The model was able to reproduce the general pattern of RA excitation and activation of its various anatomical structures in addition to a number of specific clinical observations: initial SAN activation results in two wave components that propagate in a superior and inferior direction to activate the SVC and RA respectively, and the CT plays an important role in leading electrical activation in the inferior direction [14]. As our model did not assign specific

electrophysiological properties to the CT, our results, suggest that the CT's role as a specialized conducting structure can be partially attributed to its anatomical location, electrototonic coupling to the SAN and its elongated superior-inferior shape. Contrast this to the minor role played by BB in our simulations - despite its realistic anatomical size and location. Therefore, it is important to assign specific electrophysiological properties to BB in order to simulate its role as an inter-atrial conduction pathway. Left atrial activation occurred though the inferior septum and resulted in two excitation wavefronts in the anterior and posterior LA which both moved in an inferiolateral to superiormedial direction. These results do not agree with *in vivo* human studies that suggest that the site of LA breakthrough occurs at the superior part of the LA, at the site of insertion of BB, and the excitation wavefront appears to propagate in a medial to lateral direction [14, 15]. It should be noted that the model assumes a low value for tissue conductivity and as a result the time taken for impulses to propagate from the SAN to the lateral side of the LA is much longer than that observed in clinical studies [15].

Studies on human hearts suggest that the CS forms an interatrial anatomical bridge in 93% of the population [16] and hence might play a role as a secondary interatrial conduction pathway. This is the first 3D anatomically realistic atrial model that incorporates this important feature. Initial results suggest the CS might have a role in terminating re-entrant wavefronts.

The geometry allows the study of arrhythmic behavior resulting from ectopic beats originating in the PVs and the study of the efficacy of circumferential PV ablation in terminating such ectopic impulses. Our results indicate, the lesion was effective in inducing both entrance and exist block but had no effect on arrhythmic wavefronts which already existed in the LA.

In this study it was not possible to induce a sustained episode of atrial fibrillation by introducing a single ectopic beat in the LA. Several explanations can be offered. Firstly, cardiac excitation and propagation is a chaotic phenomenon. The success of generating sustained re-entrant activity is highly sensitive to the location, size, and timing of the ectopic stimulus. Therefore, obtaining a sustained re-entrant wavefront will require numerous simulation runs for different combinations of the above factors. Although this approach is feasible for simple models (e.g. [9]) it is not practical for models using complex and irregular geometries. Secondly, many experimental studies have shown that an anatomical (e.g. scar tissue) or physiological substrate (e.g. absence of frequency dependence in the refractory period [17]) is necessary for the initiation and maintenance of re-entrant wavefronts. In this study homogenous biophysical properties were assumed and therefore the model is electrically stable. This observation is consistent with results obtained by Blanc et al. using a simplified atrial geometry [18]. It is worth noting that most published 3D models of atrial fibrillation initiated sustained re-entrant activity by rapid pacing of the atrium in the presence of a substrate for fibrillation (e.g. [8]).

A limitation of our model is that it utilizes a simple ionic model of cardiac action potentials. However this approach allowed rapid testing of the ability of our 3D model to reproduce a variety of electrophysiological phenomena. In the future we intend to incorporate detailed ionic and regional specific models into this realistic 3D geometry.

REFERENCES

[1] V. Fuster, L. E. Ryden, D. S. Cannom, H. J. Crijns, A. B. Curtis, K. A. Ellenbogen, et al., "ACC/AHA/ESC 2006 guidelines for the management of patients with atrial fibrillation," *Europace,* vol. 8, pp. 651-745, 2006.

[2] S. A. Lubitz, A. Fischer, and V. Fuster, "Catheter ablation for atrial fibrillation," *BMJ,* vol. 336, pp. 819-26, 2008.

[3] M. Haissaguerre, P. Jais, D. C. Shah, A. Takahashi, M. Hocini, G. Quiniou, et al., "Spontaneous initiation of atrial fibrillation by ectopic beats originating in the pulmonary veins," *N Engl J Med,* vol. 339, pp. 659-66, 1998.

[4] D. Harrild and C. Henriquez, "A computer model of normal conduction in the human atria," *Circ Res,* vol. 87, pp. E25-36, 2000.

[5] G. Seemann, C. Hoper, F. B. Sachse, O. Dossel, A. V. Holden, and H. Zhang, "Heterogeneous three-dimensional anatomical and electrophysiological model of human atria," *Philos Transact A Math Phys Eng Sci,* vol. 364, pp. 1465-81, 2006.

[6] M. Reumann, J. Bohnert, G. Seemann, B. Osswald, and O. Dossel, "Preventive Ablation Strategies in a Biophysical Model of Atrial Fibrillation Based on Realistic Anatomical Data," *Biomedical Engineering, IEEE Transactions on,* vol. 55, pp. 399-406, 2008.

[7] N. Virag, V. Jacquemet, C. S. Henriquez, S. Zozor, O. Blanc, J. M. Vesin, et al., "Study of atrial arrhythmias in a computer model based on magnetic resonance images of human atria," *Chaos,* vol. 12, pp. 754-763, Sep 2002.

[8] M. Rotter, L. Dang, V. Jacquemet, N. Virag, L. Kappenberger, and M. Haissaguerre, "Impact of varying ablation patterns in a simulation model of persistent atrial fibrillation," *Pacing Clin Electrophysiol,* vol. 30, pp. 314-21, 2007.

[9] S. Dokos, S. L. Cloherty, and N. H. Lovell, "Computational model of atrial electrical activation and propagation," *Conf Proc IEEE Eng Med Biol Soc,* vol. 2007, pp. 908-11, 2007.

[10] J. M. Rogers and A. D. McCulloch, "A collocation--Galerkin finite element model of cardiac action potential propagation," *IEEE Trans Biomed Eng,* vol. 41, pp. 743-57, 1994.

[11] US National Library of Medicine, National Institute of Health [Online] http://www.nlm.nih.gov/research/visible/visible_human.html

[12] T. Saito, K. Waki, and A. E. Becker, "Left atrial myocardial extension onto pulmonary veins in humans: anatomic observations relevant for atrial arrhythmias," *J Cardiovasc Electrophysiol,* vol. 11, pp. 888-94, 2000.

[13] T. N. James, "Anatomy of the human sinus node," *Anat Rec,* vol. 141, pp. 109-39, 1961.

[14] R. De Ponti, S. Y. Ho, J. A. Salerno-Uriarte, M. Tritto, and G. Spadacini, "Electroanatomic analysis of sinus impulse propagation in normal human atria," *J Cardiovasc Electrophysiol,* vol. 13, pp. 1-10, 2002.

[15] F. G. Cosio, A. Martin-Penato, A. Pastor, A. Nunez, M. A. Montero, C. P. Cantale, and S. Schames, "Atrial activation mapping in sinus rhythm in the clinical electrophysiology laboratory: Observations during Bachmann's bundle block," *J Cardiovasc Electrophysiol,* vol. 15, pp. 524-531, 2004.

[16] S. Y. Ho and D. Sanchez-Quintana, "The importance of atrial structure and fibers," *Clin Anat,* vol. 22, pp. 52-63, 2009.

[17] M. C. Wijffels, C. J. Kirchhof, R. Dorland, and M. A. Allessie, "Atrial fibrillation begets atrial fibrillation. A study in awake chronically instrumented goats," *Circulation,* vol. 92, pp. 1954-68, 1995.

[18] O. Blanc, N. Virag, J. M. Vesin, and L. Kappenberger, "A computer model of human atria with reasonable computation load and realistic anatomical properties," *IEEE Trans Biomed Eng,* vol. 48, pp. 1229-37, 2001.